Inhibiting effect of the essential oil of the *Schinus Terebinthifolius* fruits on corrosion of E24 carbon steel in 1 M HCl

N. Ouadghiri,[1,2] S. Ksama,[1] M. Benmessaoud,[1] M. Damej,[1] K. Tassaoui,[1] O. Belhoussaine,[3] H. Harhar,[3] A. El Yadini[3] and S. El hajjaji[2]

[1]Energy, Materials and Sustainable Development Team, Higher School of Technology Salé, Mohammed V University in Rabat 8007, Morocco
[2]Laboratory of Spectroscopy, Molecular Modelling Materials, Nanomaterial Water and Environment – CERNE2D, Faculty of Sciences, Mohammed V University in Rabat, Morocco
[3]Materials, Nanotechnology and Environment Laboratory (LMNE), Faculty of Sciences, Mohammed V University of Rabat, BP 1014 Rabat, Morocco
**E-mail: ouadghirinabil@gmail.com*

Abstract

This study explores the inhibitory properties of *Schinus Terebinthifolius* fruits essential oil (STFEO) on the corrosion of E24 carbon steel in a 1 M hydrochloric acid solution. Essential oil extracted from the fruits of *Schinus Terebinthifolius* (STF), underwent testing at various concentrations and temperatures through a range of methods, including utilizing weight loss measurements and electrochemical techniques, adsorption isotherms, and scanning electron microscopy (SEM). An inhibition efficiency of 90.64%, 88.36%, and 86.33% was attained when employing 1 g/L of STFEO in weight loss assessments, polarization experiments, and EIS evaluations, respectively. Observations indicated that elevating the inhibitor concentration improved its inhibitory effectiveness while raising the temperature diminished its inhibitory performance. The findings indicate that STFEO functions as a mixed-type inhibitor with a preference for the anodic effect. The STFEO adsorption adhered to the Langmuir model, and the free energy of adsorption data registered a value of −33.70 kJ/mol, signifying a physical and chemical adsorption process. Examination of the metal surface of E24 steel *via* SEM/EDS reveals the development of an inhibitory film acting as a protective barrier against corrosion, in a 1 M HCl acid solution.

Received: February 1, 2024 Published: September 17, 2024 doi: 10.17675/2305-6894-2024-13-3-28

Keywords: *Schinus Terebinthifolius, carbon steel, essential oil, corrosion, corrosion inhibition, hydrochloric acid.*

1. Introduction

E24 carbon steel is a widely used material due to its high availability, resistance to metallic degradation, and cost-effectiveness [1, 2]. It can be found in various everyday items and is

extensively used in industrial applications. However, like all metals, E24 steel is susceptible to corrosion, particularly in acidic environments like hydrochloric acid [3–6]. Consequently, corrosion poses a significant challenge in most industrialized nations [7, 8], resulting in annual economic losses amounting to hundreds of billions of dollars [9]. The substantial economic impact of corrosion has motivated scientists to develop corrosion inhibitors for acidic environments to mitigate or delay the corrosive effects on metals [10–15]. Many organic acid inhibitors are known to be effective for a range of metals and alloys [16–20]. However, these inhibitors often have adverse effects on both human health and the environment, highlighting the importance of exploring environmentally friendly alternatives.

Over the past decade, researchers have been increasingly focusing on the potential use of green inhibitors [21, 23]. These inhibitors' anti-corrosion properties attributed to their various active components, such as essential oils, exhibit moderate to high inhibitory efficiencies, ranging from 55% to over 90%, in acidic environments [24–27].

Schinus Terebinthifolius (STF) is a compact tree, typically standing between 3 to 10 meters in height, although occasionally it can reach up to 15 meters, with a trunk diameter ranging from 10 to 30 centimeters, and in some cases, as wide as 60 centimeters. This tree belongs to the *Anacardiaceae* family and is just one of the 873 species spread across 81 genera within this family**.** Native to regions including Brazil, Argentina, Paraguay, and Uruguay, STF has now established itself in various other countries, often thriving in open areas. It's commonly found along the edges of forests and on the banks of rivers. The tree produces small flowers, and its fruits often exhibit eccentric styles, with many of them being somewhat flattened and containing a single seed, known as drupes [28].

STF is sensitive to frost and thrives in tropical or subtropical climates, where it prefers moist conditions. Remarkably, it demonstrates a reasonable tolerance for both shade and drought [29].

In the context of environmental protection and the use of Moroccan flora, this study examines the potential of essential oil extracted from the STF tree to protect E24 steel from corrosion in a 1 M HCl (hydrochloric acid) environment, using weight loss measurements, electrochemical techniques, adsorption isotherms and scanning electron microscopy (SEM).

2. Material and Methods

2.1. Plant material

The STF was harvested from the region of Rabat (34°01′53.34″) in the period of February–March. Afterward, these fruits were dried at room temperature for several days.

2.2. Extraction of essential oil

The essential oil used in this research was obtained from the STF through an extraction process employing a Clevenger-type apparatus [30]. Initially, 100 grams of STF were crushed and deposited into a 1 L flask. This latter was then subjected to heating for 6 hours

to ensure the complete collection of the essential oil. The resulting mixture, comprised of essential oil and water, was subsequently dehydrated and preserved in opaque bottles. The yield of the obtained essential oil was 2.14±0.04%.

2.3. Electrodes and chemicals and test solution

Corrosion testing procedures involved electrochemical measurements conducted on E24 carbon steel sheet electrodes, each possessing a surface area of 0.78 cm² and a chemical composition specified by weight percentage as follows in Table 1.

Table 1. The chemical composition of E24 steel.

C%	Si%	P%	S%	Ti%	Co %	Cr%	Mn%	Fe%
0.11	0.24	0.021	0.16	0.011	0.009	0.077	0.47	99.046

The experiments were conducted in a corrosive hydrochloric acid medium, prepared by diluting 37% HCl with distilled water. The essential oil concentrations employed in this study ranged from 0.25, 0.5, 0.75, to 1 g/L. Additionally, the temperature was varied within the range of 293 to 323 K. For each experiment, E24 steel specimens were accurately weighed and immersed in beakers containing 50 mL of acid solutions. These solutions were prepared both without and with varying concentrations of STFEO, and the temperature was meticulously maintained using a water thermostat throughout a 5-hour immersion period. After each experiment, the E24 steel samples were polished to achieve a smooth surface. This polishing process involved the use of different grades of emery paper, namely 600, 800, 1500, and 2000.

2.4. Mass loss

The gravimetric measurements were conducted within a double-walled glass cell that featured a thermostatically controlled condenser. The E24 carbon steel samples employed in these experiments were square, measuring 1×1×0.2 cm. They underwent abrasion using different grades of emery paper (600-800-1500-2000) and were subsequently thoroughly cleaned with both distilled water and acetone. Following precise weighing, these samples were immersed for a 24-hour duration at 293 K and maintained through the use of a water thermostat. They were placed in beakers containing 100 mL of acid solutions, both without and with varying quantities of STFEO. This gravimetric testing procedure was repeated three times under identical conditions.

The corrosion rates (*CR*) of the E24 steel and the inhibition efficiency (IE_{CR}%) were calculated from the measured mass loss using the following equations [31]:

$$CR = \frac{\Delta W}{S \cdot t} \tag{1}$$

$$IE_{CR}\% = \frac{CR^0_{corr} - CR^{inh}_{corr}}{CR^0_{corr}} \cdot 100 \quad (2)$$

where the weight loss (W) is measured in grams, immersion time (t) is recorded in hours, while S is the exposed area of the sample in cm^2. The corrosion rates in the absence and presence of the STFEO are represented by CR^0_{corr} and CR^{inh}_{corr}, respectively.

2.5. Electrochemical measurements

At room temperature, EIS measurements were carried out in both blank solutions and inhibited test solutions containing various concentrations of STFEO bases, which were also utilized for weight loss measurements. The experiments were conducted over a frequency range spanning from 10 kHz to 0.01 Hz, utilizing a signal amplitude of 10 mV peak to peak, all at the corrosion potential. Z-view software automatically managed the experimental measurements, and Nyquist plots were used to display the impedance figures (Z_{real} *vs.* Z_{img}), Bode Modulus, and Phase Angle plots. Double-layer capacitance (C_{dl}) and charge transfer resistance (R_{ct}) have been determined using data from Z-view software. Inhibition efficiencies were calculated by the following Equation [32];

$$IE_{RP}\% = \frac{R^{inh}_p - R^0_p}{R^{inh}_p} \cdot 100 \quad (3)$$

where R^{inh}_p and R^0_p exhibit the charge transfer resistance in the existence and non-existence of STFEO, respectively.

Potentiodynamic polarization measurements were conducted followed by electrochemical impedance spectroscopy (EIS) studies. The same instrument setup was employed for both polarization measurements, and a scan rate of 1 mV/s was applied.

Polarization curves were generated by altering the electrode potential within the range of –800 to –100 mV (SCE *vs*. OCP). Various corrosion kinetic parameters, including corrosion potential (E_{corr}), corrosion current density (i_{corr}), as well as the anodic and cathodic Tafel slopes (b_a and b_c, respectively), were determined by extrapolating the linear Tafel segment to E_{corr} from the Tafel polarization curve. the Equation 4 was used to calculate the inhibition efficiencies [33]:

$$IE_{PDP}\% = \frac{i^0_{corr} - i^{inh}_{corr}}{i^0_{corr}} \cdot 100 \quad (4)$$

where i^{inh}_{corr} and i^0_{corr} represent the corrosion current density with and without STFEO, respectively.

2.6. Surface analysis by scanning electron microscope

A Quanta 200 FEI Company scanning electron microscope was used to examine the surface of E24 carbon steel samples in both the absence and presence of STFEO. The employed

accelerating beam has a 20 kV energy. The equipment is outfitted with a backscattered electron detector and an entire X-ray microanalysis system (EDS detector).

3. Results and Discussion

3.1. Mass loss

The effect of different STFEO concentrations on E24 carbon steel corrosion in 1 M HCl solution was evaluated using weight loss measurements at 293 K after 24 hours of immersion, and the results are shown in Table 2. The corrosion inhibition efficiency (IE_{CR}) was then calculated from the obtained corrosion rate (*CR*) values using Equation 1.

Table 2. Corrosion parameters obtained from weight loss measurements of E24 steel at various concentrations of STFEO in 1 M HCl at 293 K.

STFEO, g/L	***CR*, mg/cm^2·h**	***IE*$_{CR}$, %**
0	1.78	–
0.25	0.41	77.23
0.5	0.29	83.84
0.75	0.20	88.92
1	0.17	90.64

Table 2 illustrates the quantitative data, showing a remarkable increase in inhibition efficiency with increasing STFEO concentration at 293 K. In the absence of an inhibitor, the *CR* of E24 steel was 1.78 mg/cm^2·h. At 1 g/L of STFEO, the *CR* is equal to 0.17 mg/cm^2·h, a significant decrease in corrosion rate was observed. This concentration-dependent decrease in weight loss underlines the inhibitory effect of STFEO on mild steel corrosion in hydrochloric acid. The experimental results show that STFEO inhibits corrosion, reduces the corrosion rate, and increases the inhibition efficiency [34–37]. Notably, STFEO exhibited a remarkable inhibition efficiency, reaching 90.64% at a concentration of 1 g/L over a 24-hour exposure period.

3.2. Polarization results

3.2.1. OCP

Figure 1 illustrates the changes in the open circuit potential (*E*) over a 60-minute immersion period of E24 steel in a 1 M HCl acid solution at 293 K. These changes are observed in both the presence and the absence of various concentrations of STFEO.

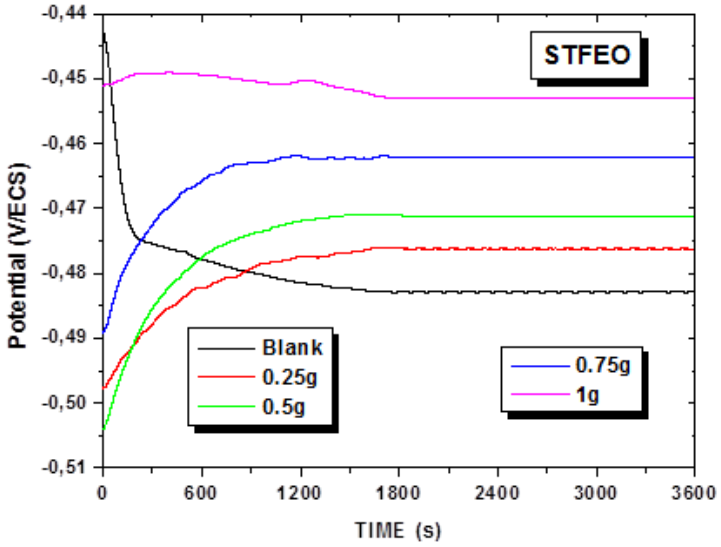

Figure 1. Evolution of the open circuit potential (OCP) as a function of exposure time of E24 steel in a 1 M HCl solution in the presence and absence of different concentrations of STFEO at 293 K.

The results indicate that as the inhibitor concentration increases, the potential decreases. The presence of the STFEO in the solution causes a shift in the curve towards the negative potential direction. This shift signifies that the inhibitor influences cathodic reaction, and it's noteworthy that the value of the corrosion potential (E_{corr}) remains relatively stable over time.

In summary, Figure 1 demonstrates that the inhibitor has a noticeable impact on the cathodic corrosion process, leading to a decrease in the potential and suggesting its effectiveness in mitigating corrosion in the studied environment. Additionally, the stability of the corrosion potential over time suggests the inhibitor's enduring protective effects.

3.2.2. Concentration effect

Figure 2 depicts the catholic and anodic polarization curves of E24 steel produced in 1 M HCl solution in the presence and absence of different concentrations of STFEO, at 293 K.

These measurements serve to elucidate how STFEO affects the corrosion behavior of E24 steel in the studied 1 M HCl solution. The inhibitory efficiency IE_{PDP}% was estimated using Equation 4.

The addition of STFEO at varied doses marginally shifts the corrosion potential (E_{corr}) towards anodic potentials, demonstrating the mixed nature of the inhibitors examined. The values of the limiting current density are lower for anodic potentials than those predicted by the inhibitor-free solution. However, increasing the concentration of inhibitor causes a considerable decrease in current density in the cathodic domain. This shows that STFEO had an effective protective effect against metal corrosion. Its extent is proportional to the concentration of the inhibitor, indicating that as the concentration grows, the protective characteristics of the produced film improve.

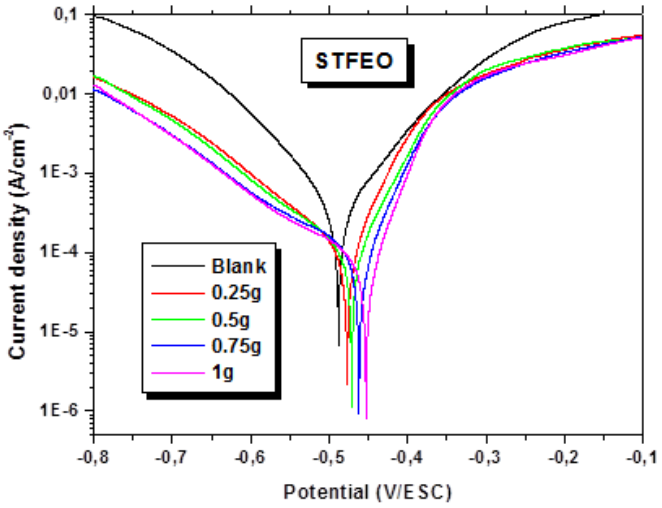

Figure 2. Potentiodynamic polarization curves of E24 steel in 1 M HCl in the presence and absence of different concentrations of STFEO at 293 K.

Table 3 provides comprehensive data, including corrosion potential (E_{corr}), corrosion current densities (i_{corr}), and inhibition efficiencies (IE_{PDP}).

Table 3 demonstrates how adding the inhibitor to the investigated medium reduces corrosion current densities (i_{corr}), which will be equal to 20.35 μA/cm^2 for a concentration of the inhibitor of 1 g/L, which suggested an increase in inhibition efficiency to 88.36%. This finding implies that the STFEO can successfully prevent the electrode from dissolving in a 1 M HCl solution [38, 39].

Table 3. Electrochemical parameters of E24 steel at 293 K and different concentrations of STFEO in 1 M HCl.

STFEO, g/L	E_{corr}, mV/SCE	i_{corr}, μA/cm^2	IE_{PDP}, %
0	–488	174.8	–
0.25	–477	43.14	75.32
0.5	–471	30.63	82.48
0.75	–461	23.63	86.29
1	–454	20.35	88.36

3.2.3. Temperature effect

Figure 3 depicts polarization curves for steel E24 at various temperatures in the presence and absence of 1 g/L of STFEO.

Analysis of this figure reveals that while the temperature increase does not affect the overall appearance of the anodic and cathodic curves, it does cause a shift in the corrosion potential towards more negative values and an increase in the corresponding corrosion current density.

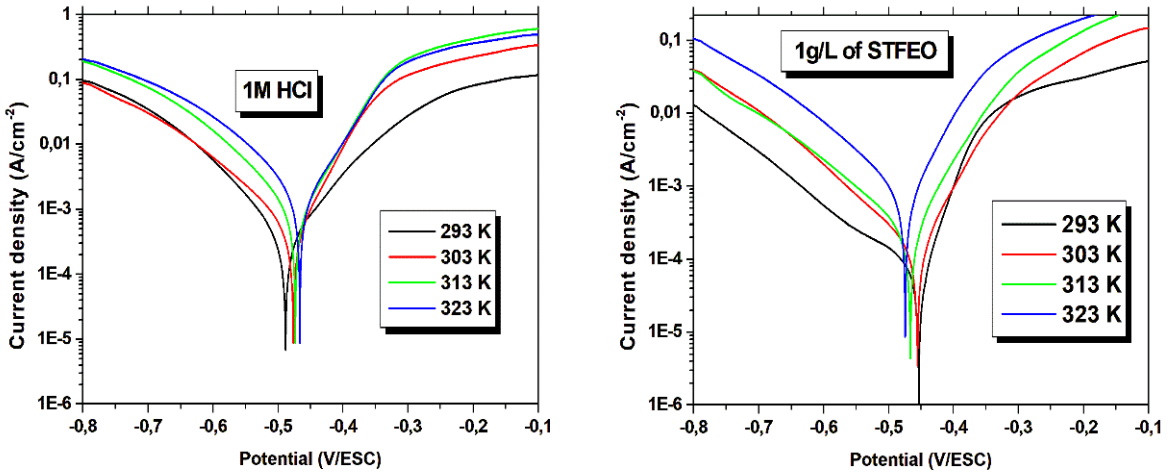

Figure 3. Polarization curves relating to the behavior of E24 steel at different temperatures without and with a 1 g/L of STFEO concentration.

Table 4 shows the effect of temperature on the electrochemical parameters that characterize the behavior of E24 steel in a 1 M HCl solution without and with 1 g STFEO, as calculated from the polarization curves.

We discovered that the corrosion current density increases with increasing temperature, whereas the inhibition efficacy reduces when the temperature rises from 293 to 323 K.

Table 4. Evolution of the electrochemical parameters of steel E24 as a function of the temperature in the absence and the presence of 1 g at STFEO.

STFEO, g/L	*T*, K	E_{corr}, mV/SCE	i_{corr}, µA/cm^2	*IE*, %
0	293	–488	174.8	–
	303	–476	234.7	–
	313	–473	341.7	–
	323	–466	735.6	–
1	293	–454	20.35	88.36
	303	–455	40.72	82.65
	313	–466	69.74	79.59
	323	–474	190.37	74.12

The thermodynamic analysis demonstrates the calculation of thermodynamic parameters and evaluates the efficacy of corrosion inhibition. Figure 4a and b show Arrhenius plots and $\ln(i_{corr}/T)$ versus $1000/T$ of E24 steel in a 1 M HCl solution without and with 1 g/L of STFEO at 293–323 K.

Table 5 shows the thermodynamic results for the activation activity as well as the predicted values of the standard activation energy (E_a), entropy (ΔH_a), and enthalpy (ΔS_a), which were calculated using the equations:

$$\ln(i_{corr}) = -\frac{E_a}{RT} + \ln A \quad (5)$$

$$i_{corr} = \frac{RT}{Nh}\exp(\frac{\Delta S_a}{R})\exp(-\frac{\Delta H_a}{RT}) \quad (6)$$

where R is the gas constant; A is the Arrhenius pre-exponential factor, N is the Avogadro number, T is the absolute temperature and h is the Plank constant.

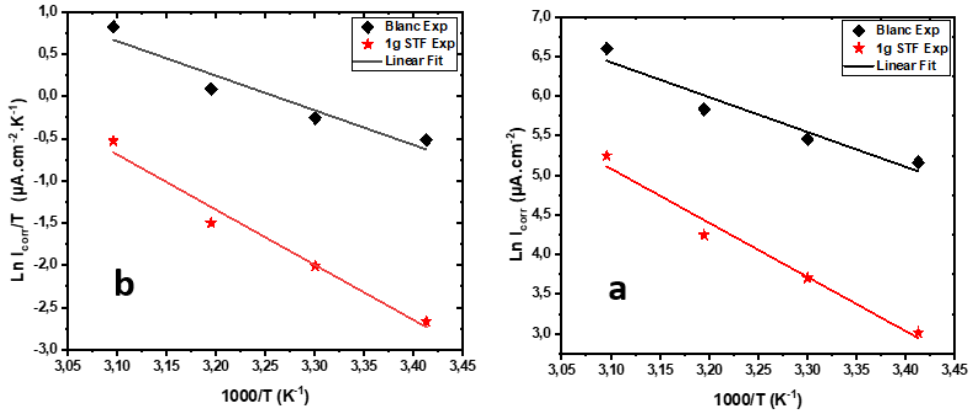

Figure 4. Arrhenius (a) and ln(i_{corr}/T) (b) plots as a function of 1000/T in a 1 M HCl solution in the absence and the presence of 1 g/L of STFEO at different temperatures.

Table 5. Activation parameters for the E24 steel dissolution in 1 M HCl in the absence and the presence of 1 g/L STFEO.

System	E_a, kJ/mol	ΔH_a, kJ/mol	ΔS_a, kJ/mol
Blank	36.61	34.05	-86.53
1 g/L STFEO	56.82	54.26	-35.06

Table 5 illustrates that the E_a values for the blank solution and STFEO (1 g/L) are 36.61 and 56.82 kJ/mol, respectively. This observation can be attributed to the formation of a protective layer on the metal surface [40]. Furthermore, the endothermic nature of the dissolution process is indicated by the positive sign of the activated enthalpy, represented by ΔH_a (*i.e.*, blank solution = 34.05 kJ/mol and STFEO 1 g/L = 54.26 kJ/mol). As Table 5 shows, this process slows down steadily when STFEO is added. Similarly, in the presence of STFEO, the ΔS_a value is negative (–35.06 kJ/mol). This indicates that the mobility of our compound within the inhibited solution is reduced [41]. It is important to note that the activated complex in the rate-determining phase indicates an association rather than a dissociation step, resulting in the fixation of the disorder. These predicted thermodynamic

properties indicate that the adsorption of BTMS onto the E24 steel surface occurs spontaneously.

3.3. Electrochemical impedance spectroscopy (EIS)

3.3.1. Concentration effect

Figure 5 depicts the graphs for Nyquist, Bode modulus, and Phase Angle for E24 carbon steel in a 1 M HCl solution at 293 K, both in the absence and presence of STFEO at various concentrations. These impedance spectra display a common feature of a single depressed semicircle (single loop), indicating a connection between the charge transfer mechanism and the corrosion process [24, 25]. The depression observed in the Nyquist semicircles may result from factors such as frequency dispersion, surface inhomogeneities and roughness, and the transport phenomena of substances [26, 27].

The Nyquist diagrams reveal similar patterns in both the presence and the absence of the inhibitor, implying that the introduction of STFEO does not alter the corrosion mechanism significantly. However, it's noteworthy that the semicircle diameters are notably larger in the presence of STFEO compared to the uninhibited solution, and this enlargement is more pronounced with increasing inhibitor concentration. The occurrence can be ascribed to the development of a protective film on the exterior (surface) of the E24 steel, leading to a reduced corrosion rate [28].

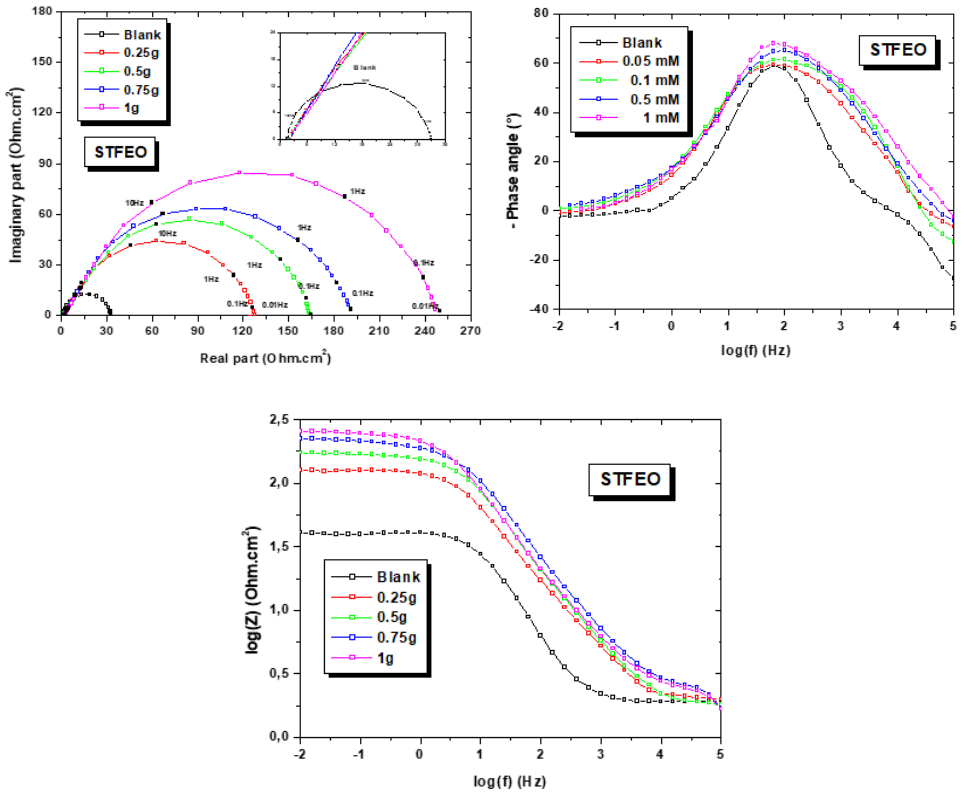

Figure 5. Nyquist, Bode modulus, and phase angle plots of E24 steel in 1 M HCl solution in the absence and presence of different concentrations of STFEO at 293 K.

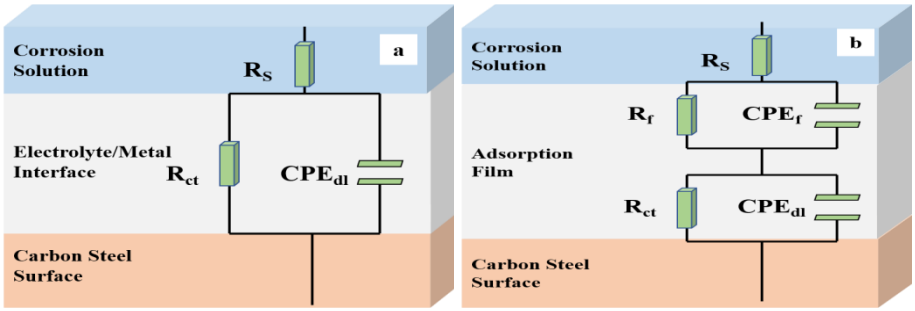

Figure 6. Electrical equivalent circuit used to simulate EIS data for the E24 steel corrosion in 1 M HCl solution: without (a) and with STFEO (b).

The spectra obtained without the inhibitor were matched by an equivalent electrical diagram including a $R_{ct}-CPE_{dl}$ circuit [42] (Figure 6a), however, the presence of the STFEO required the addition of a second R_f-C_f (Figure 6b) to model the acquired results [43]. In these equivalent electric circuits, constant phase elements (CPEs) are used instead of pure capacitors to account for the deviations of experimental EIS semicircles caused by surface inhomogeneity caused by surface roughness and impurities, inhibitor adsorption and electrode discontinuity, and so on [44]. The impedance of the CPE is described by the Equation 5 [45]:

$$Z_{CPE} = \frac{1}{y_0(jw)^{\infty}} \tag{7}$$

where w represents the angular frequency and j represents the imaginary root.

The following Equation is used to determine the double-layer capacitance using parameters acquired by fitting EIS spectra [46]:

$$C_{dl} = \left(y_0 R_p^{1-n}\right)^{1/n} \tag{8}$$

Table 6 lists the various impedance parameters determined by the Nyquist plots. The efficacy of inhibition (IE_{EIS}%) is calculated using the Equation 3.

Table 6. Parameters associated with E24 steel impedance diagrams in 1 M HCl at different concentrations of STFEO.

STFEO, g/L	R_s, Ω·cm²	R_f, Ω·cm²	C_f, μF/cm²	R_{ct}, Ω·cm²	C_{dl}, μF/cm²	IE_{EIS}, %	θ
0	1.92	–	–	31.14	511.08	–	–
0.25	1.95	–	–	126.7	125.6	74.20	0.7420
0.5	1.86	21.13	7.531	143.11	11.2	78.24	0.7824
0.75	1.66	26.69	5.962	167.91	94.8	81.45	0.8145
1	1.57	30.76	5.173	220.54	72.2	86.33	0.8633

From the results shown in Table 6, it can be deduced that increasing the inhibitor concentration tested results in a decrease in C_{dl}, which is connected to the adsorption of STFEO molecules, increasing the thickness of the film, formed on the surface of the working electrode and therefore a decrease in the degradation of the metal as well as a delay in the release of hydrogen evolution [33].

In the presence of STFEO, the resistance values of the film rise with increasing inhibitor concentration, from 21.13 Ω·cm^2 (0.5 g of STFEO) to 30.76 Ω·cm^2 (1 g of STFEO). Capacity values, on the other hand, fall from 7.53 to 5.17 μF/cm^2. They are too tiny and are mostly due to the creation of an inhibitory layer on the metal's surface. At low frequencies, the transfer resistance rises to 220.54 Ω·cm^2 for a 1 g concentration of STFEO.

The efficacy of inhibition rises as the concentration of the inhibitor rises. It is equivalent to 86.33% for 1 g of STFEO. This result is comparable to what be achieved using potentiodynamic measurements.

3.3.2. Adsorption isotherm

The adsorption isotherm can give fundamental details about how the inhibitor interacts with the E24 carbon steel surface. The Langmuir model is the most suitable and, thus, the best descriptor for the adsorption of STFEO on the E24 steel surface [38].

$$\frac{C_{inh}}{\theta} = \frac{1}{K_{ads}} + C_{inh} \tag{9}$$

C_{inh} represents the inhibitor concentration, while K_{ads} is the adsorption process's equilibrium constant. The following equation [34] describes how K_{ads} relate to the standard free energy of adsorption.

$$\Delta G^0_{ads} = -RT \ln(K_{ads} \cdot 999) \tag{10}$$

where T is the absolute temperature and R is the gas constant. The value of 999 is the concentration of water in solution in g/L.

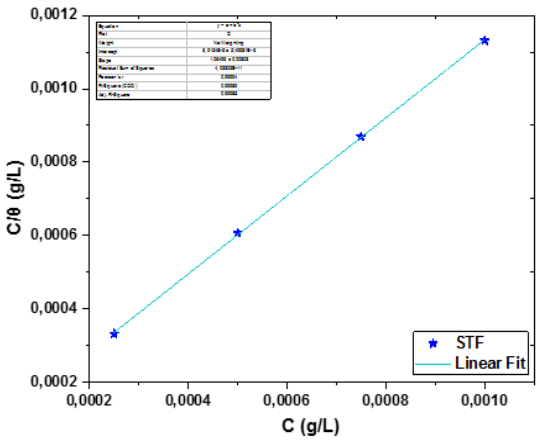

Figure 7. Langmuir's isotherm adsorption model of STFEO on the E24 steel surface in 1 M HCl at 293 K.

From Table 7, the negative value of the free enthalpy of adsorption ΔG^0_{ads} indicates that the tested inhibitor adsorbs spontaneously on the metal surface; thus, the value of ΔG^0_{ads} equals –33.70 kJ/mol, indicating that the STFEO adsorption mechanism on E24 steel in 1 M HC1 solution is both physisorption and chemisorption with a chemical [47].

Table 7. Adsorption coefficient values *K* and ΔG^0_{ads} for different concentrations of STFEO in 1 M HCl.

Inhibitor	***K***	R^2	ΔG^0_{ads}, **kJ/mol**
STFEO	$0.144 \cdot 10^5$	0.99	–33.70

3.3.3. Immersion time

Figure 8 illustrates the progression of the electrochemical impedance diagrams at the corrosion potential for 1 g/L of STFEO with respect to the duration of immersion in a 1 M HCl solution, while Table 8 summarizes the electrochemical parameters determined from the EIS curves. The electrochemical impedance diagrams exhibit an identical shape to those derived from the STFEO concentration effect, as shown in the figure. The charge transfer resistance rises with immersion time, peaking at 445.07 $\Omega \cdot cm^2$ after 24 hours. These findings suggest that the inhibitory property of STFEO stems from the creation of an extraordinarily resistant protective barrier on the E24 carbon steel surface, which prevents corrosion.

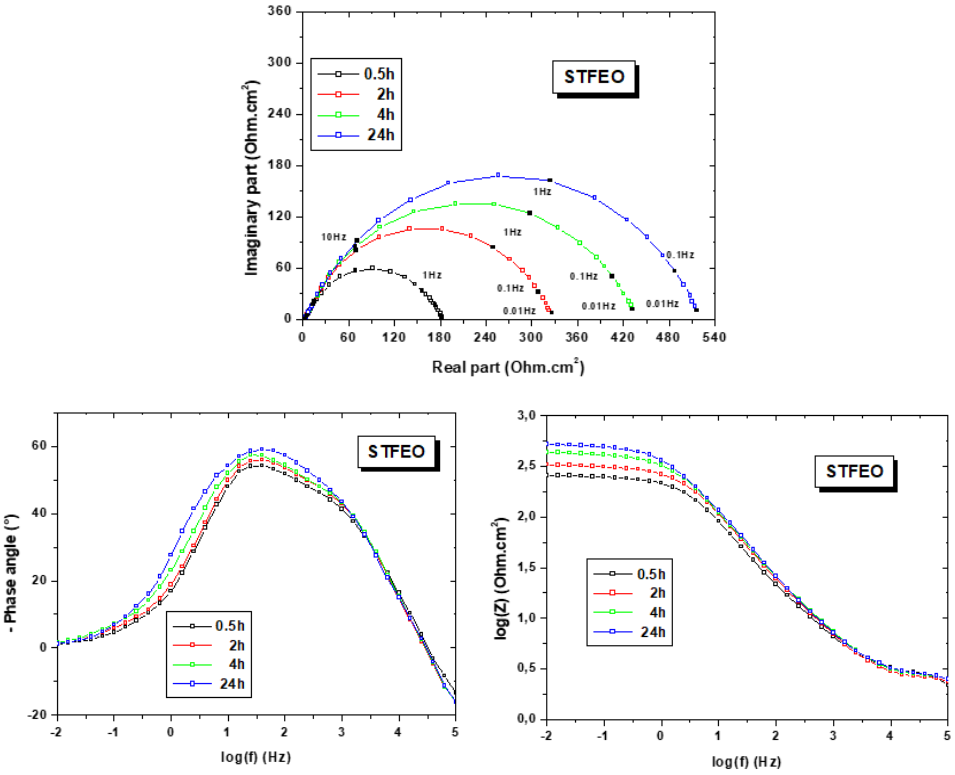

Figure 8. Nyquist, Bode modulus, and phase angle plots of E24 steel in 1 M HCl solution containing an optimal concentration of STEFEO at various immersion times at 293 K.

Table 8. Impedance parameters for E24 steel in 1 M HCl with 1 g/L of STFEO depending on the duration of immersion.

Time, h	R_s, Ω·cm^2	R_f, Ω·cm^2	C_f, µF/cm^2	R_{ct}, Ω·cm^2	C_{dl}, µF/cm^2
0.5	1.985	26.41	6.026	155.89	137.9
2	1.655	39.12	4.067	283.68	88.64
4	1.439	41.69	3.817	383.81	65.52
24	1.269	55.63	2.860	445.07	56.50

4. SEM/EDX Surface Study

Figure 9 shows the surface condition of the E24 carbon steel, observed by SEM analysis, after 24 hours of immersion in 1 M HCl solution alone (a) and with 1 g/L of STFEO (b). The existence of rust on the surface of the E24 steel (a kind of sting) clearly shows that the electrode has undergone corrosion. In contrast, in the presence of STFEO, the surface of the E24 steel immersed in HCl 1 M, has been covered by a protective film that shields it from corrosion, confirming the inhibitor's potential to prevent E24 deterioration.

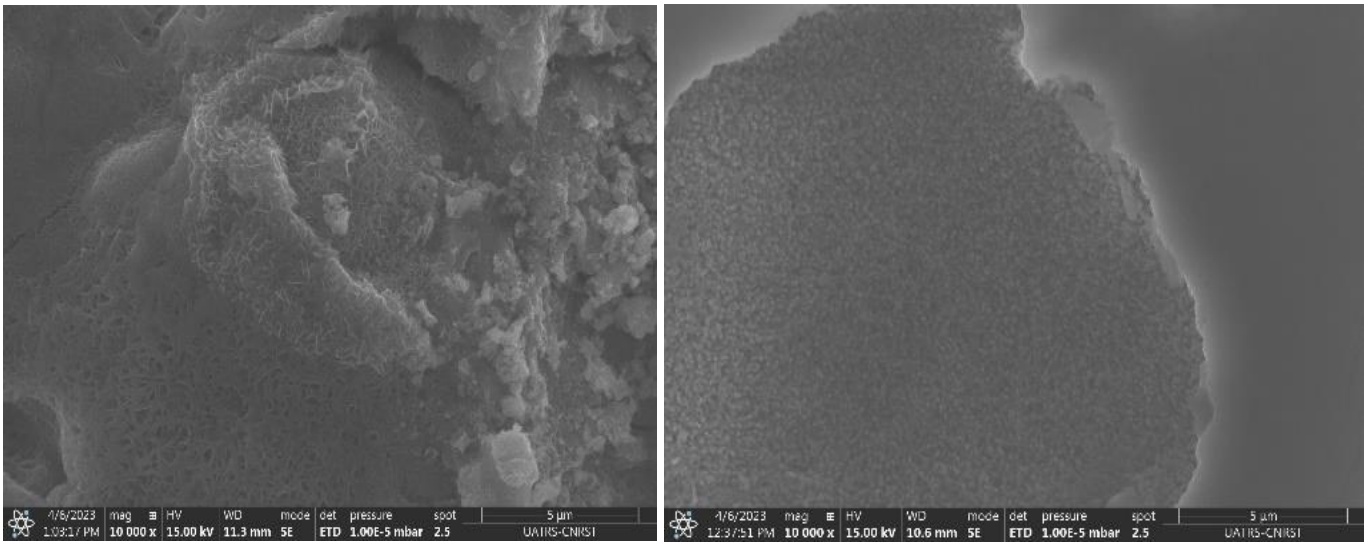

Figure 9. Micrographs showing E24 steel without inhibitor (a) and with 1 g STFEO (b) after 24 hours of immersion in 1 M HCl solution.

The EDX spectrum in 1 M HCl reveals typical peaks of certain chemical elements (iron, oxygen, and chlorine), implying the development of iron oxide/hydroxide on the metal surface. Because of the adsorbed inhibitor layer covering the E24 surface, the presence of the STFEO inhibitor implies an increase in oxygen levels.

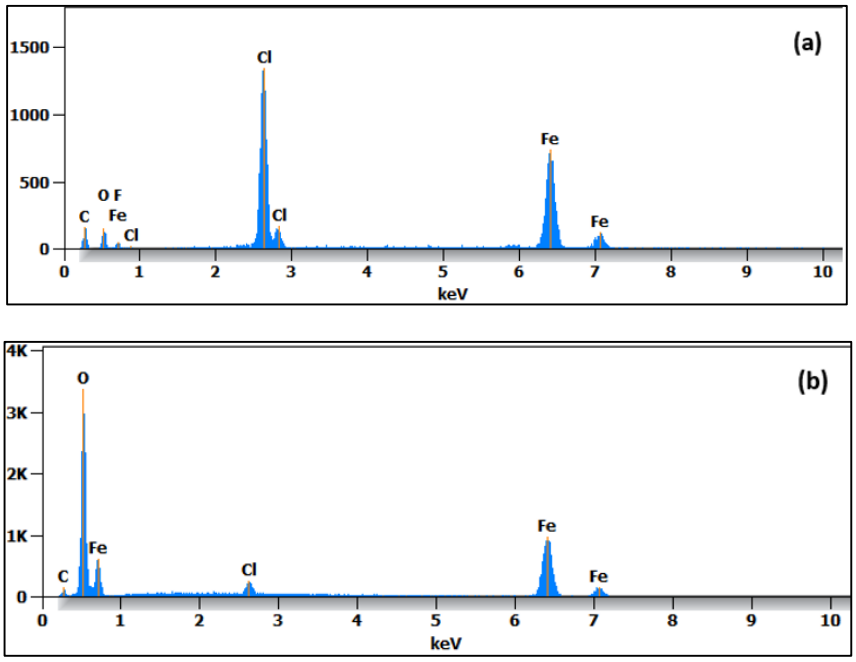

Figure 10. EDX spectra of E24 steel without inhibitor (a) and with inhibitor 1 g/L of STFEO (b) in 1 M HCl solution after 24 hours of immersion.

5. Conclusion

The key findings of this study can be summarized as follows:

1. The STFEO shows promising potential as an environmentally friendly, biodegradable inhibitor for mitigating E24 carbon steel corrosion in 1 M hydrochloric acid solutions. As confirmed by all experimental evaluations, its inhibition efficiency increases with concentration, reaching 88% at a concentration of 1 g/L.
2. Potentiodynamic polarization findings indicate that an increase in temperature leads to a decrease in inhibition efficiency and the curves suggest that STFEO primarily functions as a mixed-type inhibitor with a predominant anodic effect.
3. The EIS findings demonstrate that the inclusion of STFEO leads to a decrease in the C_{dl} value and E_{corr} an increase in the R_{ct} value, suggesting its adsorption at the interface between the metal and electrolyte.
4. The negative ΔG^0_{ads} value confirms the spontaneous nature of the adsorption process and the stability of the adsorbed double layer on the metal surface and its absolute value underscores that the interactions between the inhibitor and the metal surface are physicochemical, indicating mixed adsorption.
5. Electrochemical impedance spectroscopy (EIS) studies reveal that STFEO reduces the corrosion rate by enhancing the charge transfer resistance within the system. The equivalent circuit model effectively fits the EIS data and incorporates a constant phase element.

6. The consistency observed between gravimetric, potentiodynamic polarization, and EIS measurements strengthens the reliability of these conclusions.
7. The adsorption of STFEO molecules follows the Langmuir adsorption isotherm model. Additionally, SEM examination confirms the presence of a protective film adsorbed on the metal surface.

These findings collectively underscore the potential of STFEO as a sustainable and effective corrosion inhibitor for E24 steel in hydrochloric acid environments.

References

1. I. Chakib, N.D. Sebbar, H. Elmsellem, E.M. Essassi and Z. Abdelfettah, Comparaison des proprietes inhibitrices de corrosion de trois composes heterocycliques renfermant le motif oxo-pyrazolylidene, *Heterocycl. Chem.*, 2016, **15**, no. 1, 135–144. doi: 10.48369/IMIST.PRSM/jmch-v15i1.6999
2. M. Mobin, M. Rizvi, L.O. Olasunkanmi and E.E. Ebenso, Biopolymer from Tragacanth gum as a green corrosion inhibitor for carbon steel in 1 M HCl solution, *ACS Omega*, 2017, **2**, 7, 3997–4008. doi: 10.1021/acsomega.7b00436
3. I. Ahamad and M.A. Quraishi, Bis (benzimidazol-2-yl) disulphide: an efficient water soluble inhibitor for corrosion of mild steel in acid media, *Corros. Sci*., 2009, **51**, no. 9, 2006–2013. doi: 10.1016/j.corsci.2009.05.026
4. M. Abouchane, R. Hsissou, A. Molhi, M. Damej, K. Tassaoui, A. Berisha, A. Chraka and M. Benmessaoud, Exploratory Experiments Supported by Modeling Approaches for TGEEA New Epoxy Resin as a Contemporary Anti-corrosion Material for C38 Steel in 1.0 M HCl, *J. Fail. Anal. and Preven*., 2023, **23**, no. 4, 1765–1781. doi: 10.1007/s11668-023-01705-9
5. M. Damej, A. Molhi, H. Lgaz, R. Hsissou, J. Aslam, M. Benmessaoud, N. Rezki, H-S. Lee and D-E. Lee, Performance and interaction mechanism of a new highly efficient benzimidazole-based epoxy resin for corrosion inhibition of carbon steel in HCl: A study based on experimental and first-principles DFTB simulations, *J. Mol. Struct*., 2023, **1273**, 134232. doi: 10.1016/j.molstruc.2022.134232
6. K. Azgaou, M. Damej, S. El Hajjaji, N.K. Sebbar, H. Elmsellem, B.El Ibrahimi and M. Benmessaoud, Synthesis and characterization of N-(2-aminophenyl)-2-(5-methyl-1H-pyrazol-3-yl) acetamide (AMPA) and its use as a corrosion inhibitor for C38 steel in 1 M HCl. Experimental and theoretical study, *J. Mol. Struct*., 2022, **1266**, 133451. doi: 10.1016/j.molstruc.2022.133451
7. N. Belarbi, F. Dergal, I. Chikhi, S. Merah, D. Lerari and K. Bachari, Study of anti-corrosion activity of Algerian L. stoechas oil on C38 carbon steel in 1 M HCl medium, *Int. J. Ind. Chem*., 2018, **9**, no. 2, 115–125. doi: 10.1007/s40090-018-0143-6

8. G. Vastag, A. Shaban, M. Vraneš, A. Tot, S. Belić and S. Gadžurić, Influence of the N-3 alkyl chain length on improving inhibition properties of imidazolium-based ionic liquids on copper corrosion, *J. Mol. Liq*., 2018, **264**, 526–533. doi: 10.1016/j.molliq.2018.05.086
9. M.H. Hussin and M.J. Kassim, The corrosion inhibition and adsorption behavior of Uncaria gambir extract on mild steel in 1 M HCl, *Mater. Chem. Phys*., 2011, **125**, no. 3, 461–468. doi: 10.1016/j.matchemphys.2010.10.032
10. Q.B. Zhang and Y.X. Hua, Corrosion inhibition of mild steel by alkylimidazolium ionic liquids in hydrochloric acid, *Electrochim. Acta*, 2009, **54**, no. 6, 1881–1887. doi: 10.1016/j.electacta.2008.10.025
11. O. Benali, L. Larabi, S. Merah and Y. Harek, Influence of the Methylene Blue Dye (MBD) on the corrosion inhibition of mild steel in 0.5 M sulphuric acid, Part I: weight loss and electrochemical studies, *J. Mater. Environ. Sci*., 2011, **2**, 39–48.
12. Y. El Ouadi, N. Lahhit, A. Bouyanzer, L. Majidi, H. Elmsellem, K. Cherrak, A. Elyoussfi, B. Hammouti and J. Costa, Chemical Composition and Inhibitory Effect of Essential Oil of Lavande (Lavandula Dentata) LD on the Corrosion of Mild Steel in Hydrochloric Acid (1M), *Arabian J. Chem. Environ. Res*., 2015, **1**, no. 2, 49–65.
13. B.O. Abdelwedoud, M. Damej, K. Tassaoui, A. Berisha, H. Tachallait, K. Bougrin and M. Benmessaoud, Inhibition effect of N-propargyl saccharin as corrosion inhibitor of C38 steel in 1 M HCl, experimental and theoretical study, *J. Mol. Liq*., 2022. **354**, 118784. doi: 10.1016/j.molliq.2022.118784
14. M. Damej, R. Hsissou, A. Berisha, K. Azgaou, M. Sadiku, M. Benmessaoud, N. Labjar and S. El Hajjaji, New epoxy resin as a corrosion inhibitor for the protection of carbon steel C38 in 1M HCl. experimental and theoretical studies (DFT, MC, and MD), *J. Mol. Struct*., 2022, **1254**, 132425. doi: 10.1016/j.molstruc.2022.132425
15. Z. Lakbaibi, M. Damej, A. Molhi, M. Benmessaoud, S. Tighadouini, A. Jaafar, T. Benabbouha, A. Ansari, A. Driouich and M. Tabyaoui, Evaluation of inhibitive corrosion potential of symmetrical hydrazine derivatives containing nitrophenyl moiety in 1M HCl for C38 steel: experimental and theoretical studies, *Heliyon*, 2022, **8**, no. 3, e09087. doi: 10.1016/j.heliyon.2022.e09087
16. F. Boudjellal, H.B. Ouici, A. Guendouzi, O. Benali and A. Sehmi, Experimental and theoretical approach to the corrosion inhibition of mild steel in acid medium by a newly synthesized pyrazole carbothioamide heterocycle, *J. Mol. Struct*., 2020, **1199**, 127051. doi: 10.1016/j.molstruc.2019.127051
17. R. Rmili, H. Elmsellem, M. Ramdani, B. El Mahi, Z. Ghazi, A. Chetouani, A. Aouniti and B. Hammouti, Composition of Piper Nigrum L. Essential Oils Extracted by Classical Hydrodistillation and Microwave-assisted Hydrodistillation and Inhibitory Effect on the Corrosion of mild steel in hydrochloric acid, *J. Mater. Environ. Sci*., 2016, **7**, no. 7, 2646–2657.

18. M. Damej, S. Kaya, B. El Ibrahimi, H.S. Lee, A. Molhi, G. Serdaroğlu, M. Benmessaoud, I.H. Ali, S. EL Hajjaji and H. Lgaz, The corrosion inhibition and adsorption behavior of mercaptobenzimidazole and bis-mercaptobenzimidazole on carbon steel in 1.0 M HCl: Experimental and computational insights, *Surf. Interfaces*, 2021, **24**, 101095. doi: 10.1016/j.surfin.2021.101095
19. M. Damej, M. Benmessaoud, S. Zehra, S. Kaya, H. Lgaz, A. Molhi, N. Labjar, S. El Hajjaji, A.A. Alrashdi and H.S. Lee, Experimental and theoretical explorations of S-alkylated mercaptobenzimidazole derivatives for use as corrosion inhibitors for carbon steel in HCl, *J. Mol. Liq*., 2021, **331**, 115708. doi: 10.1016/j.molliq.2021.115708
20. F. Bouhlal, A. Mazkour, H. Labjar, M. Benmessaoud, M. Serghini-Idrissi, M. El Mahi, El M. Lotfi, S. E Hajjaji and N. Labjar, Combination effect of hydro-alcoholic extract of spent coffee grounds (HECG) and potassium Iodide (KI) on the C38 steel corrosion inhibition in 1M HCl medium: Experimental design by response surface methodology, *Chem. Data Collect*., 2020, **29**, 100499. doi: 10.1016/j.cdc.2020.100499
21. O.K. Abiola, and Y. Tobun, Cocos nucifera L. water as green corrosion inhibitor for acid corrosion of aluminium in HCl solution, *Chin. Chem. Lett*., 2010, **21**, no. 12, 1449–1452. doi: 10.1016/j.cclet.2010.07.008
22. R. Salghi, S. Jodeh, E.E. Ebenso, H. Lgaz, D.B. Hmamou, M. Belkhaouda, I.H. Ali, M. Messali, B. Hammouti and S. Fattouch, Inhibition of C-steel corrosion by green tea extract in hydrochloric solution, *Int. J. Electrochem. Sci*., 2017, **12**, no. 4, 3283–3295. doi: 10.20964/2017.04.46
23. M.A.I Al-Hamid, S.B. Al Baghdadi, T.S. Gaaz, A.A. Khadom E. Yousif and A. Alamiery, Green chemistry solutions: Harnessing pharmaceuticals as environmentally friendly corrosion inhibitors: A review, *Int. J. Corros. Scale Inhib*., 2024, **13**, no. 2, 630–670. doi: 10.17675/2305-6894-2024-13-2-1
24. R.S. Al-Moghrabi, A.M. Abdel-Gaber and H.T. Rahal, A comparative study on the inhibitive effect of Crataegus oxyacantha and Prunus avium plant leaf extracts on the corrosion of mild steel in hydrochloric acid solution, *Int. J. Ind. Chem*., 2018, **9**, 255–263. doi: 10.1007/s40090-018-0154-3
25. Y. El Hamdouni, F. Bouhlal, H. Kouri, M. Chellouli, M. Benmessaoud, A. Dahrouch, N. Labjar and S. El Hajjaji, Use of omeprazole as inhibitor for C38 steel corrosion in 1.0 M H_3PO_4 medium, *J. Fail. Anal. and Preven*., 2020, **20**, no. 2, 563–571. doi: 10.1007/s11668-020-00862-5
26. Z. Akounach, A. Al Maofari, A. El Yadini, S. Douche, M. Benmessaoud, B. Ouaki, M. Damej and S.E. Hajjaji, Inhibition of mild steel corrosion in 1.0 M HCl by water, hexane and ethanol extracts of pimpinella anisum plant, *Anal. Bioanal. Electrochem*., 2018, **10**, no. 11, 1506–1524.
27. Y.N. Otaifah, K. Hussein, M. Benmessaoud and S. El Hajjaji, Study of the inhibitory effect of the Jasminum sambac extract on the corrosion of dental amalgam in saliva media, *J. Int. Dent. Med. Res.*, 2017, **10**, no. 2, 222–232.

28. P.F. Stevens, Angiosperm phylogeny website.[WWW document] URL http://www.mobot.org/MOBOT/research. APweb/[accessed on 15 January 2012], 2012.
29. E. Weber, Invasive plant species of the world: a reference guide to environmental weeds, *Cabi*, 2017, p. 581.
30. O. Belhoussaine, C. El Kourchi, H. Harhar, A. Bouyahya, A. El Yadini, F. Fozia A. Alotaibi, R. Ullah and M. Tabyaoui, Chemical composition, antioxidant, insecticidal activity, and comparative analysis of essential oils of leaves and fruits of schinus molle and *Schinus Terebinthifolius*, *Evidence-based Complementary and Alternative Medicine*, 2022, **2022**, no. 1, 4288890. doi: 10.1155/2022/4288890
31. K. Chkirate, K. Azgaou, H. Elmsellem, B. El Ibrahimi, N.K. Sebbar, El H. Anouar, M. Benmessaoud, S. El Hajjaji and E.M. Essassi, Corrosion inhibition potential of 2-[(5-methylpyrazol-3-yl) methyl] benzimidazole against carbon steel corrosion in 1 M HCl solution: Combining experimental and theoretical studies, *J. Mol. Liq*., 2021, **321**, 114750. doi: 10.1016/j.molliq.2020.114750
32. M. Damej, H. Benassaoui, D. Chebabe, M. Benmessaoud, H. Erramli, A. Dermaj, N. Hajjaji and A. Srhiri, Inhibition effect of 1, 2, 4-triazole-5-thione derivative on the Corrosion of Brass in 3% NaCl solution, *J. Mater. Environ. Sci*., 2016, **7**, no. 3, 738–745.
33. K. Tassaoui, A. Al-Shami, M. Damej, A. Molhi, O. Mounkachi, and M. Benmessaoud, Contribution to the corrosion inhibitors of copper-nickel (Cu-30Ni) in 3% NaCl solution by two new molecules of triazole: Electrochemical and theoretical studies, *J. Mol. Struct*., 2023, **1291**, 135836. doi: 10.1016/j.molstruc.2023.135836
34. I.A. Annon, K.K. Jlood, N. Betti, T.S. Gaaz, M.M. Hanoon, F.F. Sayyid, A.M. Mustapha and A.A. Alamiery, Unlocking corrosion defense: investigating Schiff base derivatives for enhanced mild steel protection in acidic environments, *Int. J. Corros. Scale Inhib*., 2024, **13**, no. 2, 727–749. doi: 10.17675/2305-6894-2024-13-2-5
35. N.S. Abtan, A.E. Sultan, F.F. Sayyid, A.A. Alamiery, A.H. Jaaz, T.S. Gaaz, S.M. Ahmed, A.M. Mustafa, D.A. Ali and M.M. Hanoon, Enhancing corrosion resistance of mild steel in hydrochloric acid solution using 4-phenyl-1-(phenylsulfonyl)-3-thiosemicarbazide: A comprehensive study, *Int. J. Corros. Scale Inhib*., 2024, **13**, no. 1, 435–459. doi: 10.17675/2305-6894-2024-13-1-22
36. A. Mohammed, H.S. Aljbori, M.A.I. Al-Hamid, W.K. Al- Azzawi, A.A.H. Kadhum and A. Alamiery, *N*-Phenyl-*N′*-[5-phenyl-1,2,4-thiadiazol-3-yl]thiourea: corrosion inhibition of mild steel in 1 M HCl, *Int. J. Corros. Scale Inhib*., 2024, **13**, no. 1, 38–78. doi: 10.17675/2305-6894-2024-13-1-3
37. M.H. Abdulkareem, A.A. Gbashi, B.A. Abdulhussein, M.M. Kadhum, A.A.H. Alamiery and W.K. Al-Azzawi, Investigating the corrosion inhibitory properties of 1-benzyl-4-imidazolidinone on mild steel in hydrochloric acid: a thorough experimental and quantum chemical study, *Int. J. Corros. Scale Inhib*., 2024, **13**, no. 1, 411–434. doi: 10.17675/2305-6894-2024-13-1-21

38. M.V. Fiori-Bimbi, P.E. Alvarez, H. Vaca and C.A. Gervasi, Corrosion inhibition of mild steel in HCL solution by pectin, *Corros. Sci*., 2015, **92**, 192–199. doi: 10.1016/j.corsci.2014.12.002
39. A. Ehsani, M. Nasrollahzadeh, M.G. Mahjani, R. Moshrefi and H. Mostaanzadeh, Electrochemical and quantum chemical investigation of inhibitory of 1,4-Ph$(OX)_2(Ts)_2$ on corrosion of 1005 aluminum alloy in acidic medium, *J. Ind. Eng. Chem*., 2014, **20**, no. 6, 4363–4370. doi: 10.1016/j.jiec.2014.01.045
40. K. Tassaoui, M. Damej, A. Molhi, A. Berisha, M. Errili, S. Ksama, V. Mehmeti, S. El Hajjaji and M. Benmessaoud, Contribution to the corrosion inhibition of Cu–30Ni copper–nickel alloy by 3-amino-1, 2, 4-triazole-5-thiol (ATT) in 3% NaCl solution. Experimental and theoretical study (DFT, MC and MD), *Int. J. Corros. Scale Inhib*., 2022, **11**, 221–244. doi: 10.17675/2305-6894-2022-11-1-12
41. B.O. Abdelwedoud, M. Damej, K. Tassaoui, A. Berisha, H. Tachallait, K. Bougrin, V. Mehmeti and M. Benmessaoud, Inhibition effect of N-propargyl saccharin as corrosion inhibitor of C38 steel in 1 M HCl, experimental and theoretical study, *J. Mol. Liq*., 2022, **354**, 118784. doi: 10.1016/j.molliq.2022.118784
42. A. Bousskri, A. Anejjar, R. Salghi, S. Jodeh, R. Touzani, L. Bazzi and H. Lgaz, Corrosion control of carbon steel in hydrochloric acid by new eco-friendly picolinium-based ionic liquids derivative: electrochemical and synergistic studies, *J. Mater. Environ. Sci*., 2016, **7**, no. 11, 4269–4289.
43. I.B. Obot, D.D. Macdonald and Z.M. Gasem, Density functional theory (DFT) as a powerful tool for designing new organic corrosion inhibitors. Part 1: an overview, *Corros. Sci*., 2015, **99**, 1–30. doi: 10.1016/j.corsci.2015.01.037
44. G. Bahlakeh, A. Dehghani, B. Ramezanzadeh and M. Ramezanzadeh, Highly effective mild steel corrosion inhibition in 1 M HCl solution by novel green aqueous Mustard seed extract: Experimental, electronic-scale DFT and atomic-scale MC/MD explorations, *J. Mol. Liq*., 2019, **293**, 111559. doi: 10.1016/j.molliq.2019.111559
45. Y. Qiang, L. Guo, H. Li and X. Lan, Fabrication of environmentally friendly Losartan potassium film for corrosion inhibition of mild steel in HCl medium, *Chem. Eng. J*., 2021, **406**, 126863. doi: 10.1016/j.cej.2020.126863
46. P. Dohare K.R. Ansari M.A. Quraishi and I.B. Obot, Pyranpyrazole derivatives as novel corrosion inhibitors for mild steel useful for industrial pickling process: experimental and quantum chemical study, *J. Ind. Eng. Chem*., 2017, **52**, 197–210. doi: 10.1016/j.jiec.2017.03.044
47. G. Aziate, A. El Yadini, H. Saufi, A. Almaofari, A. Benhmama, H. Harhar, S. Gharby and S. El Hajjaji, Study of jojoba vegetable oil as inhibitor of carbon steel C38 corrosion in different acidic media, *J. Mater. Environ. Sci*., 2015, **6**, no. 7, 1877–1884.

♦ ♦ ♦